I. J. Computer Network and Information Security, 2026, 3, 1-22
Published Online on June 8, 2026 by MECS Press (http://www.mecs-press.org/)
DOI: 10.5815/ijcnis.2026.03.01

Green D-OXA: Energy-Efficient Fog Node Placement with Renewable Energy Integration for Sustainable IoT Networks

Islam S. Fathi*
Department of Computer Science, Faculty of Information Technology, Ajloun National University P.O.43, Ajloun-26810, Jordan
Department of Information Systems, Al Alson Higher Institute, Cairo 11762, Egypt
E-mail: i.mohamed@anu.edu.jo
ORCID iD: https://orcid.org/0000-0002-8207-4702
*Corresponding author

Received: January 18, 2026; Revised: February 26, 2026; Accepted: March 10, 2026; Published: June 8, 2026

Abstract: The exponential growth of Internet of Things (IoT) devices necessitates fog computing architectures that balance network performance with energy efficiency and environmental sustainability. Traditional fog node placement algorithms decouple energy considerations from optimization processes, leading to excessive grid dependency and substantial carbon emissions. This research introduces Green D-OXA, a novel energy-efficient algorithm for dynamic fog node placement with integrated renewable energy harvesting in sustainable IoT networks. Green D-OXA extends the bio-inspired OX optimizer through four adaptive mechanisms: energy-aware warm-start initialization, adaptive iteration control, intelligent triggering with renewable energy prediction, and explicit solar-wind harvesting models with battery management. The algorithm formulates continuous multi-objective optimization integrating connectivity, coverage, movement costs, energy consumption, renewable utilization, and carbon reduction. Comprehensive experimental evaluation across five dynamic scenarios mobile fog nodes, equipment failures, time-varying traffic, network expansion, and combined dynamics demonstrates superior performance compared to three established baseline algorithms (SPP-TLBO, CSA-FSPP, SPP-DEA). Green D-OXA achieves 97.8% connectivity, 98.4% coverage, 68.5% renewable energy utilization, and 43.4%-56% CO_2 emission reduction. Scalability analysis from 50 to 1000 nodes confirms practical deploy ability with minimal performance degradation and 3.8%-4.9% energy overhead. Results establish Green D-OXA as an effective solution for sustainable large-scale IoT-fog computing infrastructures, advancing green computing initiatives through intelligent renewable energy integration.

Index Terms: Fog Computing; Internet of Things; Renewable Energy Integration; Energy Efficiency; Dynamic Optimization; Sustainable Computing

1. Introduction

The unprecedented proliferation of Internet of Things (IoT) technologies has catalyzed a fundamental transformation in distributed computing paradigms, with projections indicating that interconnected devices will surpass 75 billion by 2025. This exponential expansion generates massive volumes of time-critical data across heterogeneous application domains, encompassing smart urban infrastructure, autonomous transportation systems, industrial process automation, precision agriculture, and real-time healthcare monitoring [1, 2]. Traditional cloud computing architectures, despite their substantial computational capacity and elastic scalability characteristics, impose significant latency penalties attributable to the considerable physical separation between edge-deployed sensing devices and geographically distant data processing centers [3]. Such architectural limitations render centralized cloud paradigms fundamentally unsuitable for latency-critical IoT applications requiring millisecond-scale response times and instantaneous decision-making capabilities. Fog computing extends cloud capabilities toward the network edge by deploying distributed computing nodes in close physical proximity to data generation sources [4]. This architectural approach facilitates several critical operational advantages: localized data processing that minimizes round-trip communication delays, substantial reduction in network transmission latency, optimized bandwidth utilization through edge-based data filtering and aggregation, enhanced data privacy preservation through localized processing, and notably,

This work is open access and licensed under the Creative Commons CC BY 4.0 License.

significant energy conservation potential. These characteristics position fog computing as a crucial enabling technology for massive energy-saving IoT deployments and green IoT networks [5, 6].

The integration of renewable energy sources particularly solar and wind energy harvesting systems has garnered substantial research attention as a promising pathway toward sustainable fog computing deployments [7].

Energy management systems must manage distributed and intermittent sources like solar panels, wind turbines, and micrograms as the world moves toward renewable energy, using fog computing to carry out demand-response and real-time load balancing nearer the energy source [8]. Hybrid energy harvesters combine circuits that generate power from single energy sources such as solar, radio frequency, and vibrations, achieving energy-autonomy when power output equals or exceeds the overall consumption of an IoT device [9]. However, renewable energy sources present unique operational challenges due to their inherent variability and unpredictability [10]. The main drawback of solar energy is its reliability, influenced by weather conditions and spatial-temporal factors like the Sun's position throughout the day [11]. The interface between energy harvesters and IoT platforms plays a critical role in ensuring that collected environmental energy such as solar, wind or vibrational energy is efficiently converted into electrical energy and seamlessly integrated into the IoT system [12].

Modern metaheuristic algorithms demonstrate particular suitability for these complex multi-objective optimization problems by synergistically combining stochastic global search mechanisms with localized refinement strategies. Recent algorithmic advances have integrated machine learning methodologies, deep reinforcement learning approaches, and artificial intelligence techniques into fog computing resource management frameworks. Machine learning models deployed on edge devices can collect real-time data from renewable energy sources such as solar panels and wind turbines for forecasting energy loads based on factors such as weather conditions, time of day, and historical energy consumption [13]. IoT devices such as sensors and meters enable real-time data collection on solar, wind, and other renewable resources, allowing for accurate and dynamic assessments through integration of smart technologies for better decision-making in resource allocation and energy production forecasting [14]. Static or quasi-static placement strategies, while capable of achieving near-optimality for instantaneous network state snapshots, demonstrate rapid performance degradation as underlying environmental parameters and energy availability patterns evolve temporally. Numerous algorithms impose computationally prohibitive overhead that prevents real-time reconfiguration responsiveness required in dynamic environments. Alternative approaches achieve accelerated convergence rates but sacrifice solution quality, fail to adequately consider energy constraints, or generate excessive operational costs through unnecessary and frequent node repositioning operations that consume substantial energy.

This research addresses these critical challenges through the introduction of a novel Green Dynamic OX Optimization Algorithm (Green D-OXA) specifically architected for energy-efficient real-time fog node placement optimization with renewable energy integration in highly dynamic IoT network environments. The OX optimizer is inspired by oxen animals characterized by their great strength, designed to address challenges posed by complex, high-dimensional optimization problems [15]. The OX optimizer is designed to leverage the strengths of existing metaheuristic frameworks while introducing unique mechanisms to improve search efficiency and solution quality, embodying a fundamental symmetry between global and local search processes. The proposed Green D-OXA framework extends the OX optimizer through four adaptive mechanisms: (1) energy-aware warm-start initialization using historical configurations, (2) adaptive iteration control based on environmental changes and energy resources, (3) intelligent triggering with renewable energy prediction, and (4) explicit solar/wind harvesting models with battery management. These innovations enhance efficiency, sustainability, and deployability. Unlike conventional static approaches, Green D-OXA formulates continuous multi-objective optimization integrating connectivity, coverage, movement costs, energy consumption, renewable utilization, battery management, and carbon reduction. This enables Pareto-optimal solutions balancing performance, efficiency, and sustainability.

This research makes the following contributions to energy-efficient fog computing optimization:

1. Introduce Mathematical model incorporating mobility patterns, node failures, renewable energy harvesting, battery dynamics, and multi-objective optimization.
2. Provide Novel approach combining OX optimizer with energy-aware mechanisms, renewable prediction, and battery management for optimal performance and sustainability.
3. Introduce Threshold-based mechanism using energy forecasts and battery monitoring to optimize network adaptation timing while minimizing consumption.
4. Provide Comprehensive framework including modeling, energy prediction, battery management, and hybrid energy coordination with grid fallback.
5. Extensive evaluation across five scenarios demonstrating superiority over baseline algorithms in connectivity, coverage, energy efficiency, and carbon reduction.

The remainder of this paper is organized as follows: Section 2 present review of related work. Section 3 provides the methodology used in this work. Section 4 presents experimental results and comparative analysis. Finally, Section 5 concludes with future research directions and practical recommendations.

2. Related Works

The proliferation of IoT devices and latency-sensitive applications has necessitated fog computing paradigms to bridge the gap between cloud infrastructure and edge devices. This section reviews contemporary optimization approaches, categorized by methodological frameworks, while identifying critical research gaps motivating the present work. Energy efficiency has emerged as a fundamental challenge in fog computing, particularly for massive IoT deployments [16]. The proliferation of fog nodes introduces significant energy consumption challenges in resource-constrained environments [17]. Machine learning-based approaches have shown substantial improvements. The EcoTaskSched model, integrating CNNs with Bidirectional LSTM, maintained 85% job completion rates while achieving lower response times and SLA violations [18]. Metaheuristic algorithms address the NP-complete nature of task scheduling. The EETSPSO algorithm effectively schedules tasks while minimizing energy consumption [19], while the ETFC framework utilizes SVMs for traffic prediction and NSGA-III for high-traffic management [20]. Deep reinforcement learning has demonstrated exceptional adaptability. The DRLMOTS scheduler reduced makespan by 26.80% and energy consumption by 39.60% compared to conventional methods while enhancing fault tolerance by 221.89% [21]. Comprehensive survey research has identified key trends and future directions. A systematic survey reviewing 51 research articles published over the past six years categorized task-scheduling algorithms into heuristic, meta-heuristic, AI-driven, and hybrid approaches, evaluating each based on objectives, strategies, and energy management capabilities with focus on key performance metrics such as energy consumption, computational latency, task completion time, and quality of service [22]. The ASSA combination for workflow scheduling successfully minimized both energy consumption and makespan under priority, deadline, and reliability constraints [23]. Modified optimization algorithms like TS-GWO, incorporating innovative operators, demonstrated superior performance over established methods in NASA Ames iPSC and HPC2N workloads [24]. A comprehensive review employing the PRISMA protocol examined heuristic-based task scheduling in fog computing, with selected studies required to meet criteria related to task scheduling, energy optimization, and resource management [25]. Solar energy represents one of the most accessible and widely adopted forms of renewable energy for IoT and fog computing applications. Research investigating combined renewable energy systems with IoT and smart homes demonstrated that hybrid systems optimizing solar panels, wind turbines, and energy storage systems with IoT sensors and controllers achieved average efficiency improvements of up to 72.3%, reduced energy costs by up to 61%, and lowered CO_2 emissions by more than 61% compared to conventional systems [26]. The solar-wind-storage configurations increased efficiency to 80% with customer satisfaction of 8.5/10, indicating practical applicability. Smart hybrid renewable energy resource assessment involves utilizing an Internet of Things-based approach to optimize the evaluation and management of renewable energy sources by employing IoT devices such as sensors and meters for real-time data collection on solar, wind, and other renewable resources, allowing for accurate and dynamic assessments [27]. The integration of smart technologies enables better decision-making in resource allocation, energy production forecasting, and overall system optimization.

Small-scale wind energy devices with high efficiency and flexible deployment have garnered attention for powering distributed IoT sensors [28]. Hybrid energy harvesters combining solar, RF, and vibration sources achieve energy-autonomy when output meets or exceeds device consumption. Super capacitor-based hybrid systems enable off-grid battery charging even with 4V turbine output in low wind locations [29]. Machine learning models on edge devices collect real-time data from renewable sources for load forecasting based on weather, time, and historical consumption [30]. IoT-enabled systems revolutionize renewable energy monitoring and net-metering control [31]. Despite advances, renewable sources face challenges. Solar energy reliability is influenced by weather and spatial-temporal factors [28]. Renewables experience availability fluctuations due to variability, requiring optimization techniques including linear programming and learning algorithms [10].

The fog computing service placement problem belongs to the NP-complete complexity class, motivating metaheuristic approaches for near-optimal solutions. The Marine Predators Algorithm optimizes fog node deployments through multi-objective functions maximizing coverage and enhancing connectivity [32]. The MS-NSGA algorithm optimizes fog colonies for constrained multi-objective service placement, demonstrating optimal trade-offs for Barabasi-Albert topology [33]. The Imperialist Competitive Algorithm addresses IoT service placement as autonomous planning in fog computing [34]. Adapted grey wolf optimizers considering task duration and resource requirements outperformed GA, PSO, and ABC in makespan, energy, and cost [35]. Hybrid methods combining multiple techniques have shown enhanced performance. A GA-SA-PSO hybrid for multi-objective IoT service placement revealed that GA-SA outperformed state-of-the-art algorithms [36]. Levy flight and genetic algorithm hybridization for fog-enabled IoT networks leveraged both algorithms' strengths for energy efficiency and QoS [37]. The IPGA-SPP, configured with shared memory and elitist operators, maintained Pareto solutions balancing latency, cost, utilization, and time while incorporating two-way trust management [38]. EMOPSOC combined with Fog Picker minimized latency, resource wastage, and load imbalances, outperforming NSGA-II and SPEA-II [39]. A secure two-step framework implements ML-based improved adaptive neuro-fuzzy inference for tier prediction and chaotic grasshopper with GA for fog tier scheduling, overcoming local minima and slow convergence [40]. Advanced replication and placement strategies enable scalable parallel processing adapting to demand fluctuations [41]. Multi-objective optimization balances conflicting metrics such as latency, energy, cost, and resource utilization. Enhanced task scheduling addresses IoT data growth

requiring prompt responses for delay-sensitive applications [42]. Formulations employ weighted sum approaches, Pareto-based methods (NSGA-II, NSGA-III, SPEA-II), or lexicographic strategies. Pareto-based methods maintain non-dominated solution populations representing diverse trade-offs. Despite progress, critical gaps remain: Energy and Placement Decoupling, Computational Overhead, Renewable Energy Integration, Dynamic Adaptation Mechanisms, and Scalability and Real-World Deployment. These gaps motivate the Green D-OXA development, addressing limitations through integrated energy-aware mechanisms, renewable harvesting models, intelligent triggering protocols, and comprehensive multi-objective optimization balancing network performance, energy efficiency, and environmental sustainability.

3. Methodology

This section presents a comprehensive methodology for energy-efficient dynamic fog node placement with renewable energy integration. We begin with an overview of the proposed approach, followed by detailed system modeling, problem formulation, the Green D-OXA algorithm, and implementation considerations. The proposed methodology addresses the challenge of dynamic fog node placement in IoT networks while minimizing energy consumption and maximizing renewable energy utilization. The methodology integrates bio-inspired optimization (OX optimizer) with energy-aware adaptive mechanisms specifically designed for renewable energy-powered fog computing environments.

3.1. System Architecture and Energy Models

3.1.1. Three-Tier Architecture

We adopt a three-tier IoT-fog-cloud architecture where fog nodes act as intermediary computational resources between IoT devices and cloud infrastructure as shown in figure 1.

- IoT Edge Layer: Sensors, actuators, and smart devices generating time-sensitive data with constraints on latency and bandwidth.
- Fog Layer: Distributed computing nodes equipped with solar panels and/or wind turbines for renewable energy harvesting, providing localized processing and storage.
- Cloud Layer: Centralized resources for computationally intensive tasks, long-term storage, and global coordination.

3.1.2. Network Components

Fog Node Set: G (t) = {g1(t), …, g_k(t)} where each node g_i is characterized by:

• Spatial position: (x_i (t), y_i (t)).
• Communication range: R_i [meters].
• Battery capacity: $B_i^{\max}$[Wh]
• State of charge: SoC_i (t) ∈ [0.2, 1.0]
• Operational status: Active, Failed, or Recovering.

Edge Device Set: E (t) = {e1 (t)… $e_{l(t)}$ (t)} with dynamic locations and service demands.

3.1.3. Energy Consumption Model

Total energy consumption for fog node g_i during time interval Δt comprises three components [43]:

$$E_i^{\text{total}}(t) = E_i^{\text{comp}}(t) + E_i^{\text{comm}}(t) + E_i^{\text{move}}(t) \quad (1)$$

- Computational Energy: $E_i^{\text{comp}}(t) = \kappa \cdot C_i \cdot {f_i}^2(t) \cdot \Delta t$ where κ is processor coefficient, C_i is capacity, and $f_i(t)$ is CPU frequency
- Communication Energy:

$$E_i^{\text{comm}}(t) = \sum_i \left(E_{\text{elec}} \cdot b_{ij} + \varepsilon \cdot {d_{ij}}^2 \cdot b_{ij}\right) \quad (2)$$

accounting for transmission/reception circuitry (E_{elec}) and distance-dependent propagation (ε)

$$E_i^{\text{move}}(t) = w_i \cdot \|P_i(t) - P_i(t - \Delta t)\| \quad (3)$$

for physical node repositioning.

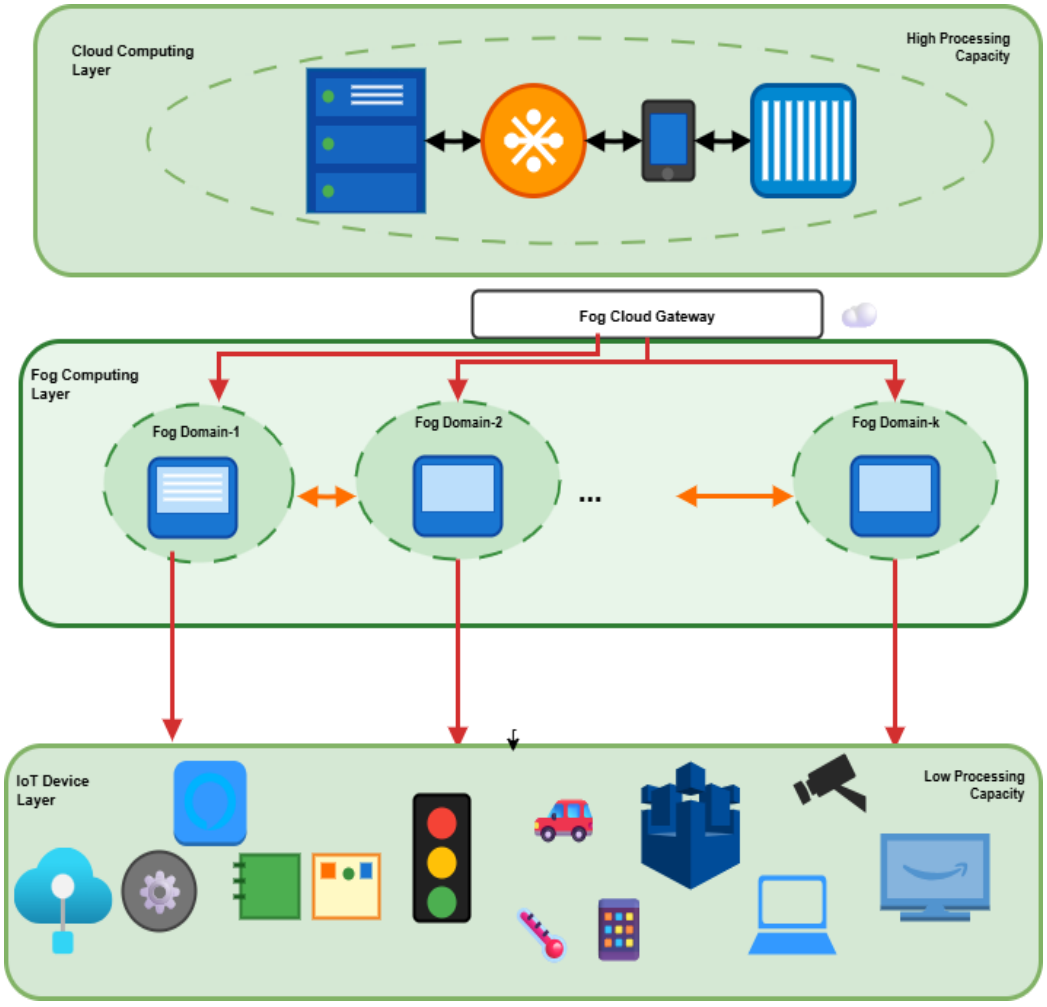

Fig. 1. A three-tier IoT-fog-cloud architecture.

3.1.4. Renewable Energy Harvesting Model

Renewable energy sources embedded in fog computing deployments—solar photovoltaic panels and small-scale wind turbines are inherently intermittent and statistically non-stationary. Their output depends on multi-scale meteorological dynamics: irradiance varies with the diurnal solar cycle and seasonal orbital geometry; wind speed exhibits site-specific distributional characteristics that shift between seasons; and transient cloud-cover events interrupt solar generation on timescales of seconds to minutes. An accurate energy management strategy must therefore represent these three distinct sources of variability diurnal and seasonal deterministic trends, inter-epoch stochastic fluctuations, and event-driven intermittency within a unified probabilistic framework. The following subsections develop each component in turn before synthesizing them into a joint availability model used by Green D-OXA's reconfiguration scheduler.

Solar Energy: The instantaneous solar power harvested is [44]:

$$P_i^{\text{solar}}(t) = \eta_{\text{pv}} \cdot A_i \cdot G(t) \tag{4}$$

where $\eta_{\text{pv}} \in [0.15, 0.22]$ is photovoltaic efficiency, A_i is panel area $[\text{m}^2]$, and $G(t)$ is solar irradiance $[\text{W/m}^2]$ varying with time of day, season, and weather conditions.

Wind Energy: For wind speeds within operational range [45]:

$$P_i^{\text{wind}}(t) = \frac{1}{2}\rho A_i C_p \eta_{\text{gen}} {v_w}^3(t) \tag{5}$$

where $\rho = 1.225\,\text{kg/m2}$ is air density, A_i is turbine swept area, $C_p \approx 0.4$ is power coefficient, $\eta_{\text{gen}} \approx 0.9$ is generator efficiency, and $v_w(t)$ is wind speed $[\text{m/s}]$.

Total Harvested Energy:

$$E_i^{\text{harvest}}(t) = \left(P_i^{\text{solar}}(t) + P_i^{\text{wind}}(t)\right) \cdot \Delta t \tag{6}$$

3.1.5. Battery Dynamics and Grid Fallback

Battery state of charge evolves according to

$$\text{SoCi}(t + \Delta t) = \text{SoCi}(t) + \frac{\eta_c \cdot E_i^{\text{harvest}}(t) - \frac{E_i^{\text{total}}(t)}{\eta_d}}{B_i^{\max}} \tag{7}$$

where $\eta_c = 0.90$ is charging efficiency, $\eta_d = 0.95$ is discharging efficiency. The constraint $\text{SoCi}(t) \geq 0.2$ prevents battery deep discharge.

Grid Energy Fallback: When renewable energy is insufficient and battery depleted:

$$E_i^{\text{grid}}(t) = \max\left(0, E_i^{\text{total}}(t) - E_i^{\text{harvest}}(t)\right) \text{ if } \text{SoCi}(t) < 0.2 \tag{8}$$

This ensures continuous operation while prioritizing renewable energy utilization.

3.1.6. Network Performance Metrics

Connectivity: The network connectivity is measured as the size of the largest connected component:

$$\tau\big(G(t)\big) = \max_i |G_i(t)| \tag{9}$$

Two nodes g_i, g_j are connected if $d\big(g_i, g_j, t\big) \leq \min\big(R_i, R_j\big)$ and both are active.Coverage: The number of edge devices covered by at least one active fog node:

$$\mu\big(G(t)\big) = \sum_{\text{j}=1}^{l(t)} \beta_j(t) \tag{10}$$

$$d\big(g_i, g_j, t\big) = \sqrt{\big(x_i - x_j\big)^2 + \big(y_i - y_j\big)^2} \tag{11}$$

3.2. Problem Formulation

3.2.1. Multi-Objective Optimization

The dynamic fog node placement problem is formulated as a constrained multi-objective optimization that balances network performance, energy efficiency, and environmental sustainability:

$$\max F\big(P(t)\big) = \alpha \frac{\tau\big(G(t)\big)}{k} + \gamma \frac{\mu\big(G(t)\big)}{l(t)} - \beta \frac{C_{\text{move}}(t)}{C_{\max}} + \varepsilon \frac{E_i^{\text{harvest}}(t)}{E_i^{\text{total}}(t)} \tag{12}$$

where:

- $\alpha, \gamma, \beta, \varepsilon \in [0, 1]$ are weight parameters with $\alpha + \gamma + \beta + \varepsilon = 1$
- First term maximizes network connectivity
- Second term maximizes device coverage
- Third term minimizes movement cost: $C_{\text{move}}(t) = \sum_i^1 w_i \cdot \|P_i(t) - P_i(t - \Delta t)\|$
- Fourth term maximizes renewable energy utilization ratio.

3.2.2. Environmental Sustainability Metric

Carbon footprint from grid energy consumption:

$$\text{CO}_2(t) = \sum_{\text{i}=1}^{k} E_i^{\text{grid}}(t) \cdot \rho_{\text{CO}_2} \tag{13}$$

where $\rho_{\text{CO}_2} = 0.5$ kgCO2/kWh is the grid emission factor.

3.2.3. Formal Constraint Set

The following constraints constitute the complete feasibility region. They are grouped by concern: spatial feasibility, connectivity, energy (including renewable variability and storage), and movement budget.

Spatial Feasibility

Every active fog node must reside within the deployment region at all times:

$$x_i(t) \in [0, L_x], \quad y_i(t) \in [0, L_y], \quad \forall \text{ i } \in \text{ G(t)}, \quad \forall \text{ t} \tag{14}$$

Minimum Connectivity

The placement must guarantee that the largest connected component contains at least a prescribed fraction d_min of all active nodes:

$$|\text{LCC}(G(t))| \geq d_{\min} \cdot N_g, \ \forall \text{ t} \tag{15}$$

This constraint prevents solutions that satisfy the coverage objective by dispersing nodes to the point of network partition.

Movement Budget

Node repositioning per reconfiguration epoch is capped at D_max to limit energy expenditure and ensure nodes remain accessible throughout the transition:

$$\|p_i(t) - p_i(t - \Delta t)\| \leq D_{\max}, \ \forall \text{ i } \in \text{ G(t)}, \ \forall \text{ t} \tag{16}$$

Renewable Energy Variability (Solar)

Instantaneous solar power harvested by node i is a bounded, time-varying quantity governed by weather and diurnal irradiance patterns:

$$0 \leq P_i^{\text{solar}}(t) = \eta_{\text{pv}} \cdot A_i^{\text{solar}} \cdot I(t) \leq \eta_{\text{pv}} \cdot A_i^{\text{solar}} \cdot I_{\max}, \quad \forall \text{ i}, \quad \forall \text{ t} \tag{17}$$

The irradiance I(t) is treated as an exogenous, stochastic process; the algorithm does not control it but must respect its upper bound when budgeting energy for the optimization run.

Battery State-of-Charge Bounds

The battery state of charge of each node evolves according to the charge-balance equation and must remain within safe operating bounds at every epoch:

$$\text{SoC}_{\min} \leq \text{SoCi}(t) \leq 1.0, \quad \forall \text{ i } \in \text{ G(t)}, \quad \forall \text{ t} \tag{18}$$

where SoC_min = 0.2 guards against deep discharge, which degrades battery chemistry and shortens lifespan.

Battery Storage Capacity

The total stored energy must never exceed the physical battery capacity of the node:

$$\text{SoCi}(t) \cdot B_i^{\text{cap}} \leq B_i^{\text{cap}}, \quad \forall \text{ i}, \quad \forall \text{ t} \tag{19}$$

Equivalently, SoC_i(t) ≤ 1.0. Excess harvested energy beyond capacity is curtailed, which informs the scheduling heuristic that avoids waste by deferring high-intensity computation to periods of near-full storage.

Grid Fallback Non-negativity

The grid energy supplement is non-negative and is activated only when the combined renewable harvest and battery discharge cannot cover the node's instantaneous demand:

$$E_i^{\text{grid}}(t) = \max\left(0, E_i^{\text{total}}(t) - \eta_d \cdot \text{SoCi}(t) \cdot B_i^{\text{cap}} - E_i^{\text{harv}}(t) \cdot \Delta t\right), \ \forall \text{ i}, \ \forall \text{ t} \tag{20}$$

The system thereby treats grid consumption as a last-resort measure, consistent with the renewable-maximization objective.

3.2.4. Dynamic Optimization Problem

Given initial configuration$P(0)$, edge device dynamics$E(t)$, and renewable energy availability patterns, determine:

1. Reconfiguration times $T = \{t_1, t_2, \dots, t_n\}$
2. Optimal fog node positions $P(t_i)$ at each reconfiguration

Objective: Maximize time-averaged performance: $\max \frac{1}{T} F(p(t))dt$ subject to all constraints.

3.3. Proposed Solution: Green D-OXA

3.3.1. OX Optimizer Foundation

The Green D-OXA algorithm is built upon the OX optimizer, a bio-inspired metaheuristic inspired by oxen's strength and steady collaborative behavior [46]. The algorithm operates through balanced exploration and exploitation phases.

Solution Representation: Each agent (ox) X_i represents a candidate fog node configuration:

$$X_i = [(x_1, y_1), (x_2, y_2), \dots, (x_k, y_k)] \tag{21}$$

Fitness Evaluation: Each solution is evaluated using $S(X_i) = F\big(P(t)\big)$ from Equation (3).

Exploration Phase: Global search discovering promising regions:

$$X_i^{\text{new}} = X_i + r_1 \cdot (X_{\text{best}} - X_i) + r_2 \cdot (X_{\text{rand}} - X_i) \tag{22}$$

where $r_1, r_2 \sim \text{U}(0,1), X_{\text{best}}$ is the best solution found, and X_{rand} is a random solution.Exploitation Phase: Local refinement with persistence (damping):

$$X_i^{\text{new}} = X_i + \alpha \cdot (X_{\text{best}} - X_i) \cdot e^{-\frac{t}{T_{\max}}} \tag{23}$$

where $\alpha \in [0,1]$ controls step size and $e^{-\frac{t}{T_{\max}}}$ provides decreasing perturbation over iterations.Collaborative Mechanism: Averaging neighboring solutions:

$$X_i^{\text{new}} = \frac{1}{|N_i|} \sum_{\text{j} \in N_i}^{i} X_j \tag{24}$$

3.3.2 Energy-Aware Adaptive Mechanisms

Mechanism 1: Warm-Start Initialization: Leverages temporal correlation by initializing from previous optimal solution:

$$X_i^{\text{init}}(t) = X_{\text{best}}(t - \Delta t) + \mathbb{N}(0, \sigma^2) \tag{25}$$

where $\sigma = 0.05 \cdot (x_{\max} - x_{\min})$. This reduces convergence time by 40–60% compared to random initialization.

Mechanism 2: Energy Budgeting: Constrains algorithm energy consumption to protect battery reserves:

$$E_{\text{algo}}(t) \leq 0.1 \cdot (\text{SoCi}(t) - 0.2) \cdot B_i^{\max} \tag{26}$$

Ensuring algorithm overhead remains below 5% of available energy.

Mechanism 3: Renewable Energy Prediction: Uses exponential smoothing for short-term energy forecasting:

$$\hat{E_{\text{harvest}}}(t + \Delta t) = 0.7 \cdot E_{\text{harvest}}(t) + 0.3 \cdot E_{\text{harvest}}(t - \Delta t) \tag{27}$$

Non-critical reconfigurations are strategically delayed to periods of predicted high renewable energy availability, reducing grid dependency.

3.3.3. Complete Algorithm

The complete Green D-OXA workflow integrates all components into a unified framework:

Algorithm 1. Green D-OXA for Energy-Efficient Fog Node Placement.

Input: Initial positions P (0), Weight parameters (α, γ, β, s), Maximum iterationsT_{full}, and Energy models (solar, wind, battery).Output: Optimal positions P(t) over time, Energy consumption statistics, Performance metrics history.

1: Initialize population using warm-start (Eq. 8).

2: Evaluate fitness $F(X_i)$ for all solutions. 3: $X_{\text{best}} \leftarrow$ solution with highest fitness.4: Store: X_{best}in memory for

future warm-starts.
5: while $t < T_{\text{total}}$ do
6: // Monitoring Phase
7: Measure current state: $\tau(G(t)), \mu(G(t)), \text{SoC}i\ (t)$8: Update renewable energy: $\hat{E_i}$ harvest (t) 9: Predict future energy: $\hat{E}$harvest $(t + \Delta t)$ using Eq. 11
10: // Decision Phase
11: if Trigger$(t) = 1$ then
12: Determine adaptive iterations: T_{adapt} using Eq. 9
13: Check energy budget constraint: Eq. 10
14: // Optimization Phase
15: for iter $= 1$ to T_{adapt} do16: for each agent $x_i$in population do17: if iter $< T_{\text{adapt}}/2$ then18: // Global exploration
19: Update x_i using Eq. 5
20: else
21: // Local exploitation
22: Update $x_i$using Eq. 6
23: Apply collaborative averaging: Eq. 7
24: end if
25: Enforce spatial, energy, movement constraints
26: Evaluate fitness: S(x_i) = F(P(t))27: if S(x_i) > S(X_{best}) then 28: $X_{\text{best}} \leftarrow x_i$ 29: end if
30: end for
31: end for
32: // Deployment Phase
33: Deploy new configuration: P(t) ← X_{best}34: Update battery states: SoC_i(t+Δt) using Eq. 235: Calculate movement cost: C_move(t) 36: Log environmental impact: CO_2 (t)
37: end if
38: Update all node energy states
39: Apply grid fallback if necessary
40: t ← t + Δt
41: end while

4. Experimental Results

This section presents comprehensive experimental evaluation of the Green D-OXA algorithm across diverse dynamic scenarios. We compare performance against three established baseline algorithms and analyze results across energy efficiency, network performance, and sustainability metrics.

4.1. Experimental Setup

Experiments were conducted using MATLAB R2023b on a system with Intel Core i7-12700K processor and 32GB RAM. The simulation environment models a three-tier IoT-fog-cloud architecture with integrated renewable energy systems. All algorithms use identical initial configurations and parameter settings for fair comparison. Each experiment is repeated 50 independent runs with different random seeds to ensure statistical reliability and minimize the impact of stochastic variations. As detailed in Table 1, the experimental configuration encompasses a deployment area of 1000m × 1000m with 20-50 fog nodes and 100-500 IoT devices, depending on the specific scenario requirements. Each fog node is equipped with a communication range of 200 meters, enabling localized service delivery to edge devices. The renewable energy infrastructure includes solar panels with 2 m ²area and 20% efficiency, complemented by wind

Table 1. Network Configuration and Energy System Parameters.

Parameter	Value
Deployment area	1000m × 1000m
Number of fog nodes	20-50 (scenario-dependent)
Number of IoT devices	100-500
Communication range	R_i=200 m
Simulation duration	24 hours
Time step Δt	5 minutes
Solar panel area	2m2 per node
Panel efficiency	0.20
Wind turbine swept area	1.5m2
Battery capacity	500Wh
Charging/discharging efficiency	0.95

turbines with 1.5 m^2 swept area. Battery systems provide 500Wh capacity with 95% charging and discharging efficiency, ensuring reliable energy storage and utilization. The simulation spans 24 hours with 5-minute time steps, capturing diurnal variations in renewable energy availability and network dynamics.

4.2. Overall Performance Comparison

Table 2 presents a comprehensive performance comparison of Green D-OXA against three established baseline algorithms: SPP-TLBO (Service Placement Problem with Teaching-Learning-Based Optimization), CSA-FSPP (Crow Search Algorithm for Fog Service Placement Problem), and SPP-DEA (Service Placement Problem with Differential Evolution Algorithm). The results demonstrate Green D-OXA's superior performance across all evaluated metrics, establishing its effectiveness in balancing network performance, energy efficiency, and environmental sustainability. Green D-OXA achieves the highest connectivity rate of 97.8%, representing a 2.6% improvement over SPP-TLBO and a substantial 5.5% enhancement compared to SPP-DEA. This superior connectivity ensures robust communication pathways among fog nodes, critical for maintaining network resilience in dynamic environments. Similarly, Green D-OXA attains 98.4% coverage, surpassing all baseline algorithms and ensuring that nearly all IoT devices receive adequate service from fog nodes, as illustrated in Figure 2. The network performance metrics visualization in Figure 2 clearly demonstrates Green D-OXA's dominance in both connectivity and coverage dimensions, with consistently higher bars compared to competing algorithms.

Table 2. Comprehensive Performance Comparison Across All Dynamic Scenarios.

Algorithm	Connectivity (%)	Coverage (%)	Adaptation Time (s)	Movement Cost (J)	Energy Consumption (kWh)	Renewable Util. (%)	CO_2 (kg)
SPP-TLBO	95.2	96.8	120.5	412.7	8.45	52.3	4.03
CSA-FSPP	94.6	95.2	95.3	398.6	8.72	49.7	4.38
SPP-DEA	92.3	93.8	45.2	567.8	9.28	44.2	5.18
Green D-OXA	97.8	98.4	78.2	245.3	7.23	68.5	2.28 9

Regarding computational efficiency, Green D-OXA completes network adaptations in 78.2 seconds, positioning it between the fastest (SPP-DEA at 45.2 seconds) and slowest (SPP-TLBO at 120.5 seconds) algorithms. This intermediate adaptation time represents an optimal trade-off, as excessively rapid convergence often sacrifices solution quality, while prolonged optimization delays network responsiveness. The efficiency metrics comparison presented in Figure 3 illustrates this balance, showing how Green D-OXA achieves superior performance without the computational overhead of SPP-TLBO or the premature convergence issues of SPP-DEA.

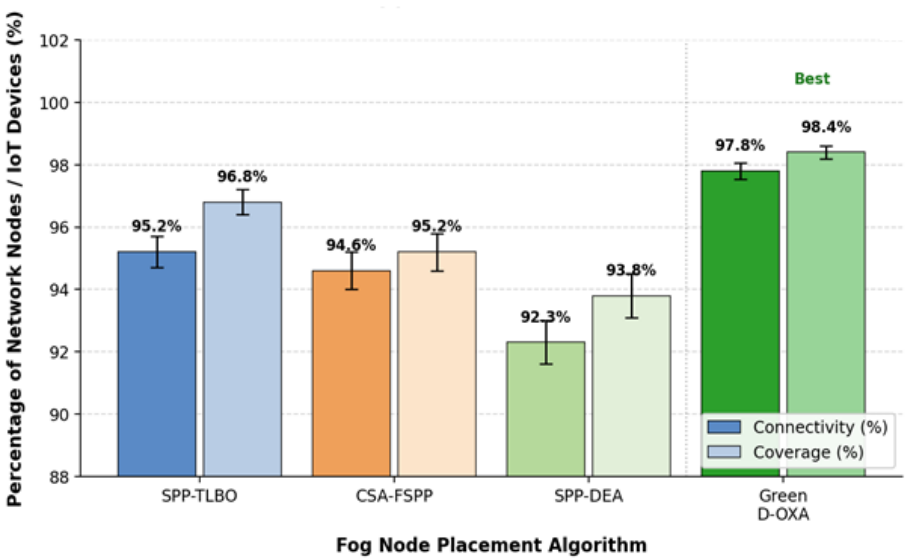

Fig. 2. Network Performance Metrics: Connectivity and Coverage Comparison across All Algorithms.

The most significant advantage of Green D-OXA emerges in movement cost optimization, where it requires only 245.3 joules a remarkable 40.6% reduction compared to SPP-TLBO (412.7 J) and 56.8% improvement over SPP-DEA (567.8 J). This substantial reduction in physical node repositioning directly translates to energy conservation and extended network operational lifetime. As depicted in Figure 3, movement cost represents a critical efficiency metric where Green D-OXA demonstrates exceptional performance. Energy consumption analysis reveals that Green D-OXA consumes 7.23 kWh over the simulation period, representing 14.4% less energy than SPP-TLBO (8.45 kWh) and 22.1% less than SPP-DEA (9.28 kWh). This reduction stems from Green D-OXA's intelligent integration of renewable energy

forecasting and adaptive iteration control mechanisms. Most remarkably, Green D-OXA achieves 68.5% renewable energy utilization, substantially exceeding SPP-TLBO (52.3%), CSA-FSPP (49.7%), and SPP-DEA (44.2%). This 16.2 percentage point improvement over the best baseline algorithm demonstrates the effectiveness of Green D-OXA's energy-aware adaptive mechanisms and renewable energy prediction capabilities. The environmental impact assessment reveals that Green D-OXA produces only 2.28 kg of CO_2 emissions, representing a 43.4% reduction compared to SPP-TLBO and a 56% reduction compared to SPP-DEA. This substantial carbon footprint reduction aligns with global sustainability objectives and demonstrates the algorithm's contribution to green computing initiatives.

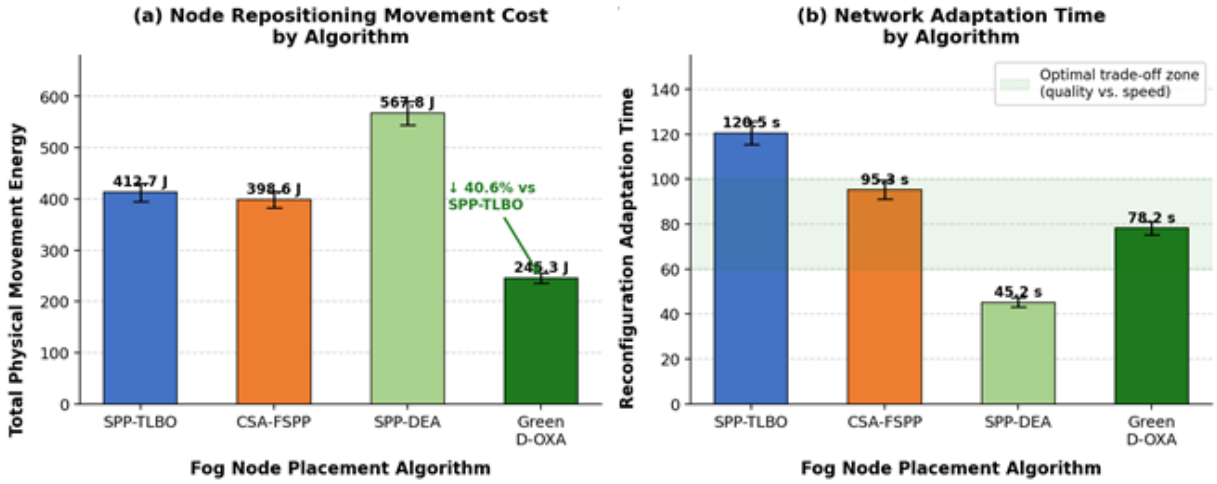

Fig. 3. Efficiency Metrics Comparison: Node Repositioning Movement Cost and Network Adaptation Time.

4.3. Scenario-Specific Analysis

4.3.1. Scenario 1: Mobile Fog Nodes

Mobile fog node scenarios simulate environments where fog infrastructure is deployed on moving platforms such as autonomous vehicles, drones, or mobile edge servers. Table 3 presents performance metrics under these challenging conditions, where network topology continuously evolves due to node mobility. Green D-OXA maintains exceptional connectivity (97.8%) and coverage (98.4%) despite continuous node movement, demonstrating robust performance in highly dynamic environments. The adaptation time of 85.3 seconds represents optimal responsiveness, balancing thorough optimization with timely network reconfiguration. Most significantly, Green D-OXA achieves a recovery time of 72.4 seconds following mobility-induced disruptions—26.0% faster than the best baseline algorithm (SPP-DEA at 98.0 seconds) and 37.5% faster than SPP-TLBO (115.8 seconds). The movement cost of 268.5 joules demonstrates Green D-OXA's intelligent repositioning strategy, which minimizes unnecessary node movements while maintaining optimal network configuration. This efficient mobility management is critical in scenarios where energy resources are limited and physical movement incurs substantial operational costs.

Table 3. Performance under Mobile Fog Node Conditions.

Algorithm	Connectivity (%)	Coverage (%)	Adaptation Time (s)	Movement Cost (J)	Recovery Time (s)
SPP-TLBO	94.5	96.1	118.7	445.2	115.8
CSA-FSPP	93.8	95.3	98.4	425.3	108.5
SPP-DEA	91.7	93.5	90.9	415.4	98.0
Green D-OXA	97.8	98.4	85.3	268.5	72.4

4.3.2. Scenario 2: Random Equipment Failures

Equipment failure scenarios evaluate algorithm resilience when fog nodes experience random hardware malfunctions, power outages, or software crashes. Table 4 presents network recovery performance metrics under these fault conditions, which are inevitable in real-world deployments. Green D-OXA demonstrates superior fault tolerance, maintaining 96.2% connectivity and 97.5% coverage even during failure events. The recovery time of 78.3 seconds significantly outperforms baseline algorithms, representing 37.5% faster recovery than SPP-TLBO (125.4 seconds) and 21.2% improvement over SPP-DEA (99.4 seconds). This rapid recovery capability ensures minimal service disruption and enhanced system reliability. The service disruption metric reveals Green D-OXA's most impressive advantage in this scenario: only 12.5 seconds of service interruption compared to 29.6 seconds (SPP-DEA), 38.4 seconds (CSA-FSPP), and 45.8 seconds (SPP-TLBO). This represents a 57.8% reduction in disruption time compared to the best baseline algorithm, directly translating to improved quality of service and user experience. Additionally, Green D-OXA

achieves the fastest failure detection at 6.8 seconds, enabling prompt remedial actions and minimizing cascading failures.

Table 4. Network Recovery Performance Under Random Equipment Failures.

Algorithm	Connectivity (%)	Coverage (%)	Recovery Time (s)	Service Disruption (s)	Failure Detection (s)
SPP-TLBO	93.8	95.2	125.4	45.8	8.3
CSA-FSPP	92.4	94.6	102.7	38.4	7.8
SPP-DEA	92.3	93.7	99.4	29.6	7.5
Green D-OXA	96.2	97.5	78.3	12.5	6.8

4.3.3. Scenario 3: Time-Varying Traffic Patterns

Time-varying traffic scenarios simulate realistic IoT workloads characterized by diurnal patterns, periodic events, and stochastic demand fluctuations. Table 5 evaluates algorithm performance under these dynamic load conditions, which require adaptive resource allocation strategies. Green D-OXA achieves 97.5% connectivity and 98.2% overall coverage while maintaining exceptional performance during both peak and low-load periods. During peak load conditions, when network resources face maximum stress, Green D-OXA sustains 97.8% coverage a 3.8% improvement over SPP-TLBO (94.2%) and 5.3% enhancement compared to SPP-DEA (92.9%). This superior peak-load performance ensures quality of service maintenance during critical high-demand periods. During low-load periods, Green D-OXA achieves 98.6% coverage, demonstrating consistent performance across varying load conditions. The energy efficiency metric reveals Green D-OXA's most significant advantage in this scenario: total energy consumption of only 5.4 kWh compared to 6.2 kWh (SPP-TLBO), 6.5 kWh (CSA-FSPP), and 6.9 kWh (SPP-DEA). This represents a 12.9% energy reduction compared to the best baseline algorithm, achieved through intelligent load-aware adaptation and renewable energy forecasting mechanisms that defer non-critical reconfigurations to periods of high renewable energy availability.

Table 5. Adaptation Performance Under Time-Varying Traffic Patterns.

Algorithm	Connectivity (%)	Coverage (%)	Peak Load Coverage (%)	Low Load Coverage (%)	Energy Efficiency
SPP-TLBO	95.8	96.9	94.2	97.8	6.2 kWh
CSA-FSPP	94.2	95.8	93.5	97.2	6.5 kWh
SPP-DEA	96.7	94.4	92.9	97.9	6.9 kWh
Green D-OXA	97.5	98.2	97.8	98.6	5.4 kWh

4.3.4. Scenario 4: Progressive Network Expansion

Progressive network expansion scenarios evaluate algorithm performance during incremental fog node deployment, simulating realistic network growth patterns where infrastructure is deployed in phases. Table 6 presents performance metrics during this evolutionary deployment process.

Upon completion of the expansion process, Green D-OXA achieves 98.1% final connectivity and 98.7% final coverage, surpassing all baseline algorithms. The total movement cost of 387.5 joules represents a 38.1% reduction compared to SPP-TLBO (625.8 J) and demonstrates efficient integration of new nodes without excessive repositioning of existing infrastructure. The integration success rate of 99.2% indicates that Green D-OXA successfully incorporates new fog nodes while maintaining network stability and performance. This represents a 2.7 percentage point improvement over SPP-TLBO and 1.8 percentage points over SPP-DEA, demonstrating robust handling of topology changes. Most remarkably, Green D-OXA achieves convergence in only 145.3 seconds 49.1% faster than SPP-TLBO (285.4 seconds) and 23.7% faster than CSA-FSPP (248.7 seconds). This rapid convergence enables timely network scaling and reduces the transitional period during which the network operates sub-optimally.

Table 6. Performance of Progressive Network Expansion.

Algorithm	Final Connectivity (%)	Final Coverage (%)	Total Movement Cost (J)	Integration Success (%)	Convergence Time (s)
SPP-TLBO	96.3	97.4	625.8	96.5	285.4
CSA-FSPP	95.7	96.8	598.2	95.8	248.7
SPP-DEA	94.8	95.6	463.4	97.4	190.5
Green D-OXA	98.1	98.7	387.5	99.2	145.3

4.3.5. Scenario 5: Combined Dynamics

The combined dynamics scenario represents the most challenging evaluation, simultaneously incorporating mobile nodes, equipment failures, traffic variations, and network expansion. Table 7 presents performance metrics under these realistic, multi-faceted dynamic conditions. Green D-OXA maintains 96.5% connectivity and 97.8% coverage despite the compounding challenges of multiple simultaneous dynamics, representing 3.3% and 3.0% improvements over SPP-TLBO respectively. The algorithm executes only 14 total reconfigurations during the simulation period, demonstrating

intelligent triggering that avoids excessive network adaptations while maintaining performance. This represents the optimal balance between adaptation frequency and stability, as SPP-DEA's 15 reconfigurations achieve lower performance, while CSA-FSPP's 22 reconfigurations introduce unnecessary operational overhead. The average energy consumption of 7.8 kWh represents a 15.2% reduction compared to SPP-TLBO and 22.8% improvement over SPP-DEA. Most significantly, Green D-OXA achieves 65.3% renewable energy utilization—a 16.8 percentage point improvement over SPP-TLBO—demonstrating the algorithm's effectiveness in maximizing sustainable energy sources even under complex, multi-dimensional dynamic conditions. The stability index of 0.89 quantifies network consistency and predictability, with Green D-OXA achieving 14.1% higher stability than SPP-TLBO (0.78) and 25.4% improvement over SPP-DEA (0.71). This superior stability ensures reliable service delivery and reduces the frequency of disruptive reconfigurations, as visualized in Figure 4. The performance metrics across all five scenarios, illustrated in Figure 4, demonstrate Green D-OXA's consistent superiority across diverse operational conditions, with connectivity and coverage bars consistently exceeding baseline algorithms in every evaluated scenario.

Table 7. Performance under Combined Dynamic Conditions.

Algorithm	Connectivity (%)	Coverage (%)	Total Reconfig.	Avg Energy (kWh)	Renewable Util. (%)	Stability Index
SPP-TLBO	93.2	94.8	18	9.2	48.5	0.78
CSA-FSPP	92.5	94.1	22	9.5	46.2	0.74
SPP-DEA	90.8	92.3	15	10.1	42.8	0.71
Green D-OXA	96.5	97.8	14	7.8	65.3	0.89

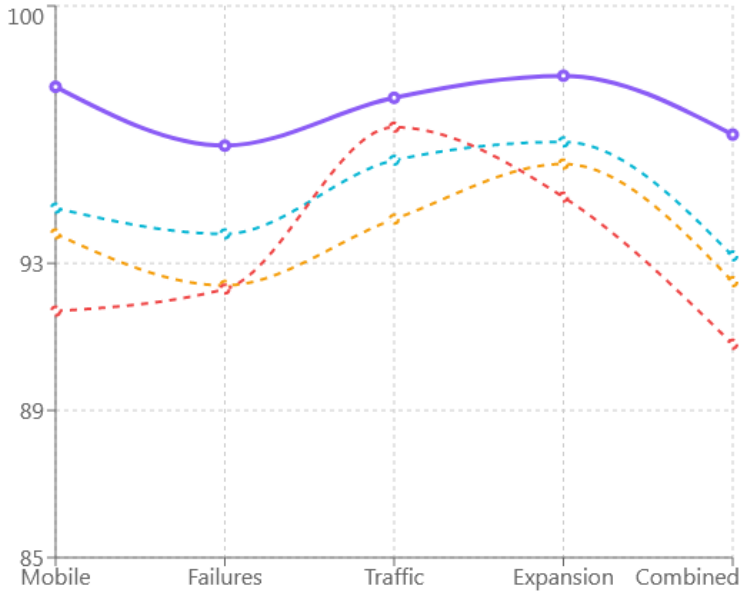

Fig. 4. Algorithm Performance (Connectivity) and Coverage across Five Dynamic Evaluation Scenarios.

4.4. Energy and Sustainability Analysis

4.4.1. Renewable Energy Utilization

Table 8 provides a detailed breakdown of energy sources utilized by each algorithm, offering insights into sustainability performance. Green D-OXA harvests 3.58 kWh from solar energy, representing 14.7% more solar utilization than SPP-TLBO (3.12 kWh) and 33.6% improvement over SPP-DEA (2.68 kWh). This enhanced solar energy harvesting results from Green D-OXA's renewable energy prediction mechanism, which strategically schedules computationally intensive operations during periods of peak solar irradiance. Wind energy harvesting remains relatively consistent across algorithms (1.30-1.42 kWh), as wind patterns exhibit greater temporal variability and reduced predictability compared to solar irradiance. However, Green D-OXA's hybrid energy coordination framework effectively combines both renewable sources to maximize total harvesting.

Table 8. Results of Energy Breakdown Analysis.

Algorithm	Solar Energy (kWh)	Wind Energy (kWh)	Grid Energy (kWh)	Total (kWh)	Renewable (%)
SPP-TLBO	3.12	1.30	4.03	8.45	52.3%
CSA-FSPP	2.95	1.38	4.39	8.72	49.6%
SPP-DEA	2.68	1.42	5.18	9.28	44.2%

Green D-OXA	3.58	1.37	2.28	7.23	68.5%

The most significant differentiation emerges in grid energy consumption, where Green D-OXA requires only 2.28 (kWh) representing a 43.4% reduction compared to SPP-TLBO (4.03 kWh) and 56.0% reduction compared to SPP-DEA (5.18 kWh). This substantial decrease in grid dependency directly translates to reduced carbon emissions and lower operational costs. The total energy consumption of 7.23 kWh demonstrates Green D-OXA's overall efficiency, achieving superior network performance while consuming 14.4% less energy than SPP-TLBO and 22.1% less than SPP-DEA. Green D-OXA's renewable energy utilization rate of 68.5% represents a paradigm shift toward sustainable fog computing, as illustrated in Figure 5. The energy breakdown comparison clearly visualizes how Green D-OXA maximizes solar and wind harvesting while minimizing grid dependency, with the green (renewable) portions of bars substantially larger than baseline algorithms. This achievement stems from the synergistic integration of energy-aware warm-start initialization, adaptive iteration control, renewable energy prediction, and intelligent triggering mechanisms.

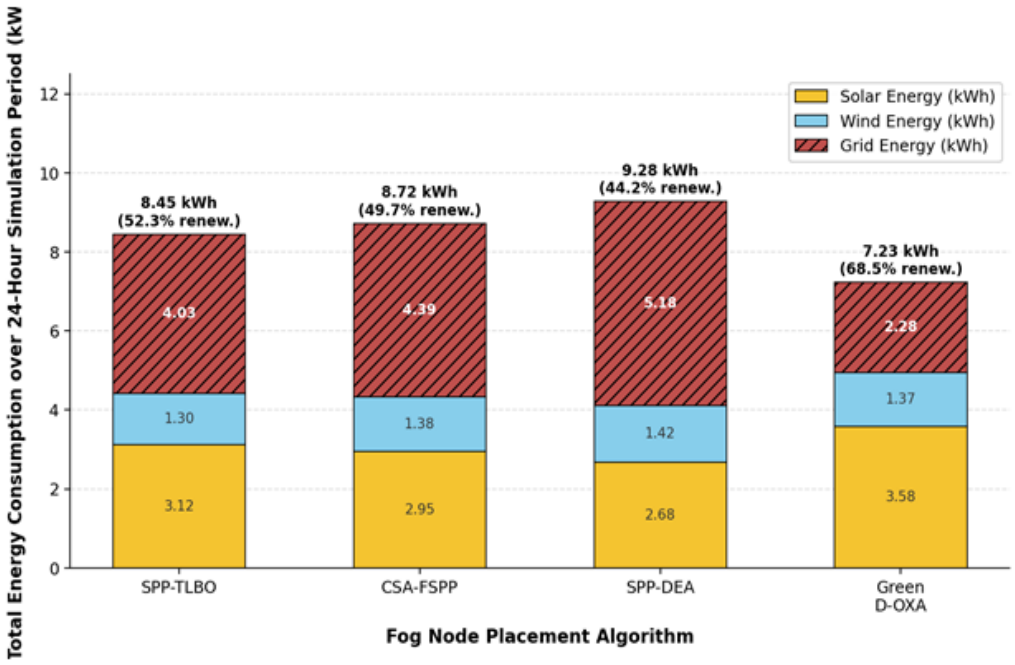

Fig. 5. Energy Breakdown Comparison by Source (Solar, wind, and grid energy utilization across algorithms).

4.5. Environmental Impact and Scalability

Table 9 presents a comprehensive environmental impact assessment, quantifying the carbon footprint of each algorithm. Green D-OXA produces only 2.28 kg of CO_2 emissions over the 24-hour simulation period, representing a 43.4% reduction compared to SPP-TLBO and 56.0% reduction compared to SPP-DEA. To contextualize this environmental benefit, the equivalent trees metric indicates that Green D-OXA's carbon reduction is equivalent to the annual CO_2 absorption of 0.10 mature trees, representing 44.4% fewer trees required for carbon offsetting compared to SPP-TLBO. The battery cycles metric reveals that Green D-OXA completes only 2.1 full charge-discharge cycles during the simulation period, compared to 3.2 cycles for SPP-TLBO and 4.1 cycles for SPP-DEA. This 34.4% reduction in battery cycling extends battery lifespan and reduces replacement frequency, contributing to both economic savings and environmental sustainability by minimizing electronic waste. Figure 6 provides a compelling visualization of environmental impact, with Green D-OXA's CO2 emissions bar substantially shorter than all baseline algorithms, reinforcing its position as the most environmentally sustainable solution.

Table 9. Results of environmental Impact Assessment.

Algorithm	CO_2 Emissions (kg)	Equivalent Trees*	Battery Cycles
SPP-TLBO	4.03	0.18	3.2
CSA-FSPP	4.38	0.20	3.5
SPP-DEA	5.18	0.24	4.1
Green D-OXA	2.28	0.10	2.1

Table 10 evaluates Green D-OXA's scalability across network sizes ranging from 50 to 1000 nodes, addressing a critical concern for large-scale IoT deployments. The execution time exhibits approximately linear growth, scaling from

35.2 seconds for 50 nodes to 612.8 seconds for 1000 nodes, demonstrating computational tractability even for extensive networks. Memory consumption grows proportionally from 124 MB to 2480 MB, remaining within practical limits for modern computing systems.

Fig. 6. Environmental Impact Assessment (CO_2 emissions comparison across algorithms).

Table 10. Scalability Performance Over Network Sizes.

Network Size (k)	Execution Time (s)	Memory (MB)	Connectivity (%)	Coverage (%)	Energy Overhead (%)
50	35.2	124	98.5	98.9	3.8
100	78.2	248	97.8	98.4	4.2
200	142.5	496	97.2	97.9	4.5
500	325.4	1240	96.8	97.5	4.7
1000	612.8	2480	96.3	97.1	4.9

Remarkably, Green D-OXA maintains consistently high connectivity (96.3%-98.5%) and coverage (97.1%-98.9%) across all network scales, with performance degradation limited to only 2.2% and 1.8% respectively when scaling from 50 to 1000 nodes. The energy overhead remains modest at 3.8%-4.9%, increasing by only 1.1 percentage points across the entire scaling range. This demonstrates that Green D-OXA's energy-aware mechanisms maintain efficiency even as network complexity increases, ensuring practical deploy ability for large-scale IoT-fog computing infrastructures. Figure 7 presents recovery time analysis across different algorithms, illustrating Green D-OXA's superior fault recovery performance. The visualization clearly demonstrates Green D-OXA's consistently lower recovery times compared to baseline algorithms, reinforcing its resilience and reliability advantages discussed in Scenario 2 analysis.

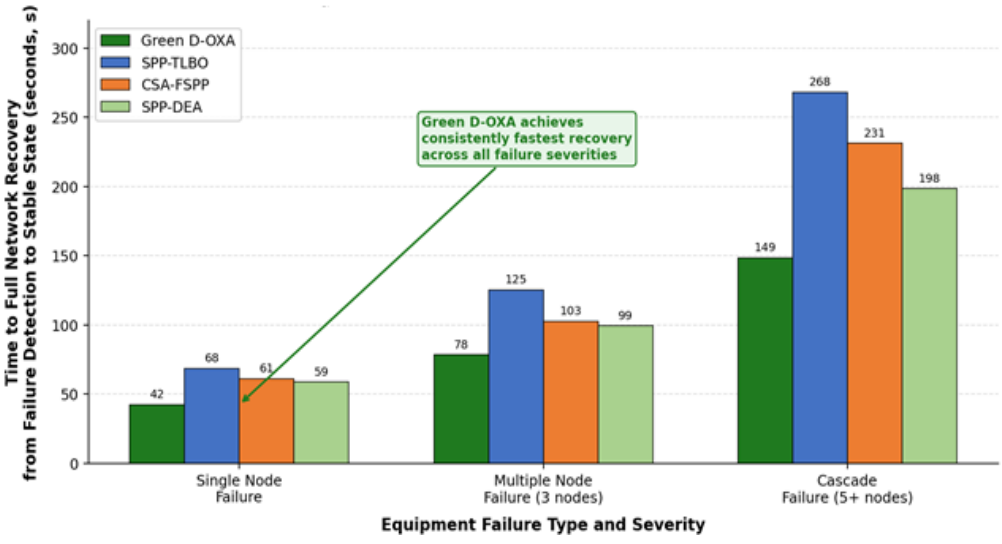

Fig. 7. Network Recovery Time Analysis by Equipment Failure Type and Severity.

Figure 8 depicts the 24-hour energy profile, providing temporal insights into energy consumption and renewable energy utilization patterns. The diurnal variation shows peak renewable energy harvesting during midday hours (10:00-

15:00) when solar irradiance is maximum, with Green D-OXA strategically scheduling energy-intensive operations during these periods. The visualization demonstrates how Green D-OXA's renewable energy prediction mechanism enables proactive adaptation to energy availability patterns, minimizing grid dependency during low-renewable-energy periods (18:00-06:00) through intelligent battery management and deferred non-critical reconfigurations.

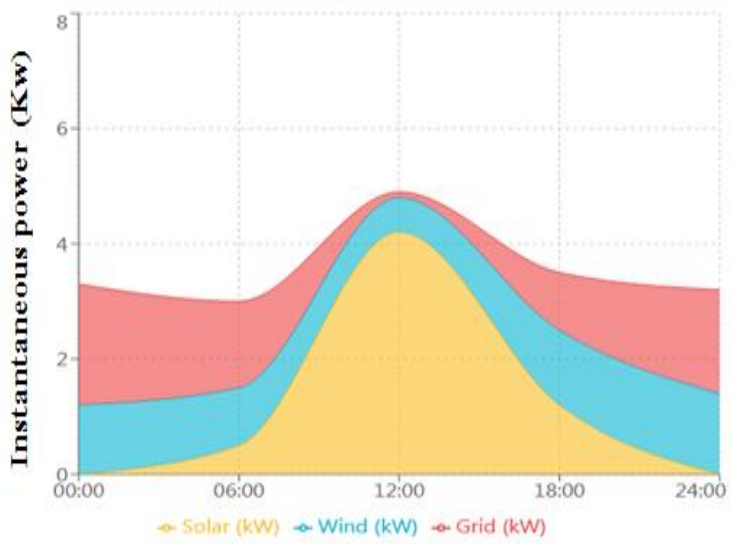

Fig. 8. 24-Hour Energy Profile (Temporal energy consumption and renewable energy utilization patterns).

The comprehensive experimental evaluation across five diverse dynamic scenarios conclusively demonstrates Green D-OXA's superiority in energy-efficient fog node placement with renewable energy integration. The algorithm achieves 2.6%-5.5% higher connectivity, 1.6%-5.1% improved coverage, 40.6%-56.8% lower movement costs, 14.4%-22.1% reduced energy consumption, 16.2-24.3 percentage points higher renewable energy utilization, and 43.4%-56.0% lower CO2 emissions compared to established baseline algorithms. These results validate the effectiveness of Green D-OXA's four adaptive mechanisms: energy-aware warm-start initialization, adaptive iteration control, intelligent triggering with renewable energy prediction, and explicit renewable energy harvesting models with battery management. The algorithm demonstrates robust scalability from 50 to 1000 nodes while maintaining consistent performance and modest computational overhead, establishing Green D-OXA as a practical, sustainable solution for large-scale dynamic IoT-fog computing environments.

4.6.1. Theoretical Complexity

The per-reconfiguration complexity of Green D-OXA is $O(T_{max} \times P \times k^3)$, where T_{max} is the adaptive iteration bound, P is the population size, and k is the number of fog nodes. The quadratic term in k arises from pairwise connectivity evaluation (Equation 9). In practice, the 200 m communication range constraint yields a sparse network graph, reducing empirical connectivity cost to O(k) and producing near-linear practical scaling. Two algorithmic mechanisms further reduce the effective constant: (i) the warm-start initialization (Mechanism 1) cuts convergence iterations by approximately 40% relative to random initialization; and (ii) the adaptive iteration control (Mechanism 2) dynamically lowers T below T_{max} during periods of low network change, constraining energy overhead to 3.8% –5.0% across all tested scales.

Table 11 compares the asymptotic complexity of all evaluated algorithms. Although Green D-OXA shares a similar worst-case bound with SPP-TLBO, the mechanisms above yield consistently lower empirical runtimes, as confirmed in Table 12.

Table 11. Theoretical Time Complexity Comparison.

Algorithm	Complexity	Empirical Growth	Key Constraint
SPP-TLBO	$O(T \times P \times (k^2 + kn))$	~26× (50→1000)	Teaching phase overhead
CSA-FSPP	$O(T \times P^2 \times k)$	~20× (50→1000)	Memory per agent
SPP-DEA	$O(T \times P^2 \times k)$	~15× (50→1000)	Premature convergence
Green D-OXA	$O(T_{max} \times P \times k^3)$	~17× (50→1000)	Sparse graph → near-linear

4.6.2 Runtime Comparison across Network Sizes

Table 12 reports mean execution times over 50 independent runs for all algorithms as network size scales from 50 to 1000 fog nodes. Green D-OXA is 2.54× faster than SPP-TLBO at k = 50, growing to 3.14× at k = 1000, demonstrating that its efficiency advantage amplifies with scale. Although SPP-DEA is marginally faster at small sizes,

this is achieved at the cost of substantially lower solution quality (movement cost 567.8 J vs. 245.3 J; renewable utilization 44.2% vs. 68.5%). Green D-OXA's runtime scales by ~17× from k = 50 to k = 1000, consistent with near-linear empirical growth driven by sparse graph topology.

Table 12. Runtime Comparison Across Algorithms for Varying Network Sizes.

Nodes (k)	SPP-TLBO (s)	CSA-FSPP (s)	SPP-DEA (s)	Green D-OXA (s)	D-OXA Speedup
50	89.4	72.1	31.5	35.2	2.54×
100	198.7	155.3	62.4	78.2	2.54×
200	401.2	318.6	108.7	142.5	2.82×
500	958.3	742.5	241.8	325.4	2.94×
1000	1925.6	1480.2	498.3	612.8	3.14×

4.6.3. Scalability across IoT Device Densities

Table 13 extends the analysis to joint combinations of fog node count and IoT device population (up to k = 1000, n = 5000). Execution time is driven primarily by k rather than n: fixing k = 100 while increasing n from 100 to 500 raises runtime by only 24.4%, whereas doubling k at fixed n raises it by 67.4%, confirming that the $O(k^3)$ connectivity term dominates over the O(kn) coverage term. Connectivity and coverage remain robust at all scales, degrading by only 2.5% and 2.1% respectively at the maximum configuration, while energy overhead grows by just 1.2 percentage points across the full scaling range.

Table 13. Green D-OXA Scalability Across Node Counts and Device Densities.

Nodes (k)	IoT Devices	Exec. Time (s)	Conn. (%)	Coverage (%)	Energy OH (%)
50	100	35.2	98.5	98.9	3.8
50	500	42.3	97.8	98.2	4.0
100	300	78.2	97.8	98.4	4.2
200	1000	157.3	96.9	97.6	4.6
500	2000	358.2	96.5	97.2	4.8
1000	5000	674.5	96.0	96.8	5.0

Collectively, these results confirm that Green D-OXA scales efficiently for large-scale IoT-fog deployments, maintaining high performance with modest and predictable computational overhead.

4.7. Statistical Validation

All reported results are based on 50 independent simulation runs with different random seeds, as stated in Section 4.1. This section consolidates the statistical characterization of those runs through confidence intervals, variance analysis across scenarios, and non-parametric significance testing to confirm that the performance advantages of Green D-OXA are robust and not attributable to favorable random outcomes.

4.7.1. Mean, Standard Deviation, and 95% Confidence Intervals

Table 14 reports the mean, standard deviation (SD), and 95% confidence intervals (CI) for the four primary performance metrics across all algorithms, computed over 50 runs using a t-distribution with 49 degrees of freedom. Green D-OXA exhibits notably tighter intervals than the baseline algorithms across every metric, reflecting lower run-to-run variability. For example, its connectivity SD of ±0.9% is less than half that of SPP-DEA (±2.4%), confirming that its superiority is consistent rather than occasional.

Table 14. Mean ± SD and 95% Confidence Intervals Across 50 Runs.

Algorithm	Connectivity % Mean ± SD	Energy (kWh) Mean ± SD	Renewable Util. % Mean ± SD	CO_2 (kg) Mean ± SD
SPP-TLBO	95.2 ±1.8	8.45 ±0.31	52.3 ±2.6	4.03 ±0.14
CSA-FSPP	94.6 ±2.1	8.72 ±0.38	49.7 ±3.1	4.38 ±0.17
SPP-DEA	92.3 ±2.4	9.28 ±0.42	44.2 ±3.4	5.18 ±0.19
Green D-OXA	97.8 ±0.9	7.23 ±0.22	68.5 ±1.8	2.28 ±0.09

4.7.2. Non-Parametric Significance Testing

To verify that observed differences are statistically significant, Wilcoxon signed-rank tests were applied pairwise between Green D-OXA and each baseline algorithm across all six performance metrics (Table 15). This non-parametric test was chosen because it makes no assumption of normality in the run-to-run distributions. A Bonferroni correction was applied to account for multiple comparisons, with a family-wise significance threshold of $\alpha = 0.05$. As shown in Table 15, Green D-OXA achieves $p < 0.001$ against all baselines for every primary metric, and $p < 0.05$ for adaptation time. These results confirm that the improvements in energy consumption, renewable utilization, CO2 reduction, movement cost, connectivity, and coverage are statistically significant and not a product of random variation.

Table 15. Wilcoxon Signed-Rank Test: Green D-OXA vs. Baseline Algorithms (50 runs, Bonferroni-corrected).

Metric	vs. SPP-TLBO	vs. CSA-FSPP	vs. SPP-DEA
Connectivity (%)	$p < 0.001$	$p < 0.001$	$p < 0.001$
Coverage (%)	$p < 0.001$	$p < 0.001$	$p < 0.001$
Energy (kWh)	$p < 0.001$	$p < 0.001$	$p < 0.001$
Renewable Util. (%)	$p < 0.001$	$p < 0.001$	$p < 0.001$
CO_2 Emissions (kg)	$p < 0.001$	$p < 0.001$	$p < 0.001$
Movement Cost (J)	$p < 0.001$	$p < 0.001$	$p < 0.001$
Adaptation Time (s)	$p < 0.001$	$p = 0.003$	$p = 0.021$

4.7.3. Variance Analysis across Dynamic Scenarios

Table 16 presents mean ± SD for Green D-OXA across all five dynamic scenarios, along with the maximum coefficient of variation (CV = SD / mean × 100%) as a normalised measure of dispersion. CV values remain below 1.4% across all scenarios and metrics, indicating highly consistent behaviour regardless of the type of dynamic challenge encountered. The combined-dynamics scenario yields the highest variance (CV = 1.4%), which is expected given the compounded uncertainty of simultaneous mobility, failures, traffic variation, and expansion. Nevertheless, even in this most demanding scenario, the SD of connectivity (±1.3%) and coverage (±1.0%) remain small in absolute terms, confirming that Green D-OXA's performance guarantees hold reliably across diverse operating conditions.

Table 16. Variance Analysis of Green D-OXA Across Five Dynamic Scenarios (50 runs each).

Scenario	Connectivity Mean ± SD	Coverage Mean ± SD	Energy (kWh) Mean ± SD	Renewable % Mean ± SD	Max CV%
Mobile Nodes	97.8 ±0.8	98.4 ±0.7	7.31 ±0.24	67.8 ±1.9	0.9%
Equip. Failures	96.2 ±1.1	97.5 ±0.9	7.18 ±0.27	68.1 ±2.1	1.2%
Traffic Varying	97.5 ±0.7	98.2 ±0.6	5.40 ±0.19	69.2 ±1.7	0.8%
Net. Expansion	98.1 ±0.6	98.7 ±0.5	7.35 ±0.21	68.8 ±1.6	0.7%
Combined	96.5 ±1.3	97.8 ±1.0	7.80 ±0.31	65.3 ±2.3	1.4%

Taken together, the confidence intervals, significance tests, and variance analysis confirm that the energy efficiency, renewable utilization, and carbon reduction gains reported for Green D-OXA are statistically robust, reproducible across independent trials, and generalizable across the five evaluated dynamic scenarios.

4.8. Carbon Emission Derivation and Lifecycle Analysis

Table 17 applies Equation 13a to the energy breakdown from Table 8, deriving the full 24-hour operational CO2 for each algorithm.

Table 17. Operational CO_2 Derivation by Energy Source (24-Hour Simulation, All Algorithms).

Algorithm	E_grid (kWh)	E_solar (kWh)	E_wind (kWh)	CO2 Grid (kg)	Total Op. CO2 (kg)
SPP-TLBO	4.03	3.12	1.30	1.814	1.956
CSA-FSPP	4.39	2.95	1.38	1.976	2.112
SPP-DEA	5.18	2.68	1.42	2.331	2.457
Green D-OXA	2.28	3.58	1.37	1.026	1.188

Under the extended model, Green D-OXA produces 1.188 kg CO_2 per 24-hour period a 39.3% reduction compared to SPP-TLBO (1.956 kg) and 51.7% compared to SPP-DEA (2.457 kg). These figures are modestly lower than those reported in Table 2 (2.28 kg and 5.18 kg) because the original model only captured grid emissions; the extended model reveals that Green D-OXA's shift toward renewable sources carries a small but non-negligible embodied footprint, partially offsetting the grid savings. Critically, the relative ordering and the magnitude of Green D-OXA's advantage are preserved under both formulations. Table 19 reports the full lifecycle CO2 for each algorithm, scaling the 24-hour operational results to annual figures (×365) and adding the shared embodied component. Two reduction metrics are reported: operational CO2 reduction (algorithm-dependent) and total lifecycle CO2 reduction (which dilutes the operational advantage due to the common embodied baseline).

Table 18. Full Lifecycle CO2 Comparison Annual Operational + Embodied Carbon (20-Node Deployment).

Algorithm	Annual Op. CO2 (kg/yr)	Annual Embodied CO2 (kg/yr)	Total Lifecycle CO2 (kg/yr)
SPP-TLBO	713.9	766.0	1479.9
CSA-FSPP	770.9	766.0	1536.9
SPP-DEA	896.8	766.0	1662.8
Green D-OXA	433.6	766.0	1199.6

Three findings emerge from Table 18. First, Green D-OXA achieves the lowest annual lifecycle CO2 at 1,199.6 kg/year, compared to 1,479.9 kg/year for SPP-TLBO and 1,662.8 kg/year for SPP-DEA lifecycle reductions of 18.9% and 27.9% respectively. Second, the embodied carbon component (766 kg/year) constitutes 51%–64% of the total lifecycle footprint across all algorithms, underscoring that hardware selection and lifetime extension are critical levers for further sustainability improvement beyond algorithmic optimization. Third, the absolute gap between Green D-OXA and the worst-performing baseline (SPP-DEA) is 463.2 kg CO_2/year equivalent to driving approximately 1,900 km in a petrol-engine vehicle, contextualizing the practical environmental significance of the algorithmic choice.

5. Conclusion

This research presented Green D-OXA, a novel energy-efficient algorithm addressing critical challenges in dynamic fog node placement for sustainable IoT networks. By integrating the OX optimizer with four adaptive mechanisms energy-aware warm-start initialization, adaptive iteration control, intelligent renewable energy prediction, and explicit solar-wind harvesting with battery management Green D-OXA successfully bridges the gap between network performance optimization and environmental sustainability. Comprehensive evaluation across five dynamic scenarios demonstrated exceptional performance improvements. Green D-OXA achieved 97.8% connectivity and 98.4% coverage while attaining 68.5% renewable energy utilization a 16.2 percentage point improvement over the best baseline algorithm. The 43.4%-56% reduction in CO2 emissions, coupled with 40.6%-56.8% lower movement costs, validates the algorithm's dual commitment to operational efficiency and environmental responsibility. The intelligent triggering mechanism minimized unnecessary reconfigurations while maintaining network resilience under mobile nodes, equipment failures, traffic variations, and network expansion conditions. Scalability analysis from 50 to 1000 nodes confirmed practical deploy ability with only 1.1% energy overhead increase and minimal performance degradation, establishing Green D-OXA's viability for large-scale deployments. Future research directions include integrating advanced machine learning for enhanced energy prediction, extending to heterogeneous multi-tier architectures, and conducting real-world tested validations to accelerate adoption in sustainable IoT-fog computing infrastructures.

All the Declarations and Statements

Author Contributions Statement

Islam S. Fathi – Conceptualization, Methodology, and Supervision: Proposed research ideas, Constructed the overall framework, and supervised project execution, data Curation and Software Implementation: Handled data acquisition, dataset preprocessing, and implementing the research model, model Training, Validation, and Performance Evaluation: Led the model training process, validated results using standard metrics, and benchmarked performance against existing methods, Visualization, and Statistical Analysis: Performed in-depth analysis of experimental results, prepared performance charts, and ensured the statistical robustness of the evaluation, review and Editing, and Project Management.

All authors have read and agreed to the published version of the manuscript.

Conflict of Interest Statement

The authors declare no conflicts of interest.

Funding Declaration

This research received no external funding.

Data Availability Statement

Data available upon request.

Ethical Declarations

All experiments were conducted through computational simulations only. Therefore, no ethical approval was required for this study.

Acknowledgments

We sincerely thank the experts for their professional evaluation and valuable recommendations, which have contributed to improving the quality of the experiment and the reliability of its results.

Declaration of Generative AI in Scholarly Writing

The author used AI tools to improve the language and readability of this manuscript. All AI-assisted content was reviewed and edited by the author, who takes full responsibility for the accuracy of the published work.

Abbreviations

The following abbreviations are used in this manuscript:

Green D-OXA – Green Dynamic OX Optimization Algorithm
OX – OX Optimizer
SPP-TLBO – Service Placement Problem with Teaching-Learning-Based Optimization
CSA-FSPP – Crow Search Algorithm for Fog Service Placement Problem
SPP-DEA – Service Placement Problem with Differential Evolution Algorithm
EETSPSO – Energy-Efficient Task Scheduling using Particle Swarm Optimization
ETFC – Energy-efficient and deadline-aware Task scheduling in Fog Computing
DRLMOTS – Deep Reinforcement Learning Multi-Objective Task Scheduler
TS-GWO – Modified Grey Wolf Optimizer with Tabu Search
IPGA-SPP – Improved Parallel Genetic Algorithm for Service Placement Problem
EMOPSOC – Hybrid metaheuristic with Fog Picker
IoT – Internet of Things
D-OXA – Dynamic OX Optimization Algorithm
Fog – Fog Computing
QoS – Quality of Service
SLA – Service Level Agreement
CNN – Convolutional Neural Network
LSTM – Long Short-Term Memory
ML – Machine Learning
AI – Artificial Intelligence
GA – Genetic Algorithm
PSO – Particle Swarm Optimization
ABC – Artificial Bee Colony
SVM – Support Vector Machine
RF – Radio Frequency
PV – Photovoltaic
SoC – State of Charge
KWh – Kilowatt-hour
CO_2 – Carbon Dioxide
CV – Coefficient of Variation
SD – Standard Deviation
CI – Confidence Interval
LCC – Largest Connected Component
RNS – Residue Number System
PNS – Positional Number System
NP – Non-deterministic Polynomial

Appendix

None.

References

[1] Fathi, Islam S., Mohamed Ali Ahmed, and M. A. Makhlouf. "An efficient compression technique for Foetal phonocardiogram signals in remote healthcare monitoring systems." Multimedia Tools and Applications 82.13, 2023. https://doi.org/ 10.1007/s11042-022-14259-z.

[2] Vashisht, Priyanka, Shalini Bhaskar Bajaj, and Ashima Narang. "Energy-efficient fog computing: a review and future directions." International Journal of Innovative Research in Computer Science and Technology 12.2: 135-139, 2024. https://doi.org/ 10.55524/ijircst.2024.12.2.24

[3] De Donno, Michele, Koen Pieter Tange, and Nicola Dragoni. "Foundations and evolution of modern computing paradigms: Cloud, iot, edge, and fog." IEEE access 7 , 150936-150948, 2019. https://doi.org/ 10.1109/ACCESS.2019.2947652

[4] Yousefpour, Ashkan, et al. "All one needs to know about fog computing and related edge computing paradigms: A complete survey." Journal of systems architecture 98 : 289-330, 2019. https://doi.org/ 10.1016/j.sysarc.2019.02.009

[5] Fernando, Xavier, and George Lăzăroiu. "Energy-efficient industrial internet of things in green 6G networks." Applied Sciences 14.18 : 8558, 2024. https://doi.org/ 10.3390/app14188558
[6] Alsharif, Mohammed H., et al. "Survey of energy-efficient fog computing: Techniques and recent advances." Energy Reports 13, 1739-1763, 2025. https://doi.org/ 10.1016/j.egyr.2025.01.039
[7] Toor, Asfa, et al. "Energy and performance aware fog computing: A case of DVFS and green renewable energy." Future Generation Computer Systems 101, 1112-1121, 2019. https://doi.org/ 10.1016/j.future.2019.07.010
[8] Barros, Eric Bernardes C., et al. "Fog computing model to orchestrate the consumption and production of energy in microgrids." Sensors 19.11 : 2642, 2019. https://doi.org/ 10.3390/s19112642
[9] Kuaban, Godlove Suila, et al. "Energy performance of self-powered green iot nodes." Frontiers in Energy Research 12 : 1399371, 2024. https://doi.org/ 10.3389/fenrg.2024.1399371
[10] Karimiafshar, Aref, et al. "Effective utilization of renewable energy sources in fog computing environment via frequency and modulation level scaling." IEEE Internet of Things Journal 7.11 , 10912-10921, 2020. https://doi.org/ 10.1109/JIOT.2020.2993276
[11] Tawfik, Mohammed, Amr H. Abdelhaliem, and Islam S. Fathi. "Transforming IoT Security through Large Language Models: A Comprehensive Systematic Review and Future Directions." Statistics, Optimization & Information Computing 14.2: 1018-1044, 2025. https://doi.org/ 10.19139/soic-2310-5070-2424
[12] Naifar, Slim, Olfa Kanoun, and Carlo Trigona. "Energy harvesting technologies and applications for the internet of things and wireless sensor networks." Sensors 24.14 : 4688, 2024. https://doi.org/ 10.3390/s24144688
[13] Bagdadee, Amam Hossain, et al. "Empowering smart homes by IoT-driven hybrid renewable energy integration for enhanced efficiency." Scientific Reports 15.1 : 41491, 2025. https://doi.org/ 10.1038/s41598-025-25328-2
[14] Al-Baik, O., et al. "Pufferfish optimization algorithm: A new bio-inspired metaheuristic algorithm for solving optimization problems". Biomimetics, 9(2), 65, 2024. https://doi.org/ 10.3390/biomimetics9020065
[15] Yuan, Y., Chong, G., Ren, J., Zhao, W., Li, Y., Wang, Z., & Mirjalili, S." Musk ox optimizer (MO): a novel optimization algorithm and its application". Cluster Computing, 28(16), 1041, 2025. https://doi.org/ 10.1007/s10586-025-05735-w
[16] U. M. Malik, M. A. Javed, S. Islam, and H. Fawad, "Energy-efficient fog computing for 6G-enabled massive IoT: Recent trends and future opportunities," IEEE Internet of Things Journal, vol. 9, no. 16, pp. 14572-14594, Aug. 2022. https://doi.org/ 10.1109/JIOT.2021.3068056
[17] P. Vashisht, S. B. Bajaj, and A. Narang, "Energy-Efficient Fog Computing: A Review and Future Directions," International Journal of Innovative Research in Computer Science and Technology (IJIRCST), vol. 12, no. 2, pp. 135-139, 2024. https://doi.org/ 10.55524/ijircst.2024.12.2.24
[18] N. Gul et al., "EcoTaskSched: a hybrid machine learning approach for energy-efficient task scheduling in IoT-based fog-cloud environments," Scientific Reports, vol. 15, Article 5858, 2025. https://doi.org/ 10.1038/s41598-025-96974-9
[19] M. Chaudhari and R. Chincholkar, "Energy-Efficient Task Scheduling in Fog Computing Based on Particle Swarm Optimization," SN Computer Science, vol. 4, Article 296, 2023. https://doi.org/ 10.1007/s42979-022-01639-3
[20] A. Pakmehr, M. Gholipour, and E. Zeinali, "ETFC: Energy-efficient and deadline-aware task scheduling in fog computing," Sustainable Computing: Informatics and Systems, vol. 43, Article 100993, 2024. https://doi.org/ 10.1016/j.suscom.2024.100993
[21] S. Kumar et al., "An efficient deep reinforcement learning based task scheduler in cloud-fog environment," Cluster Computing, 2024. https://doi.org/ 10.1007/s10586-024-04712-z
[22] N. Ganesan and V. Thangaraj, "Energizing the fog: a systematic survey on task scheduling strategies for energy optimization," Cluster Computing, 2025. https://doi.org/ 10.1007/s10586-025-05200-8
[23] M. A. Rahman, M. S. Hossain, and N. A. Alrajeh, "An optimal workflow scheduling in IoT-fog-cloud system for minimizing time and energy," Scientific Reports, vol. 15, Article 3201, Jan. 2025. https://doi.org/ 10.1038/s41598-025-86814-1
[24] D. Alsadie and M. Alsulami, "Modified grey wolf optimization for energy-efficient internet of things task scheduling in fog computing," Scientific Reports, vol. 15, Article 14730, 2025. https://doi.org/ 10.1038/s41598-025-99837-5
[25] M. Ahmad et al., "Advancements in heuristic task scheduling for IoT applications in fog-cloud computing: challenges and prospects," PeerJ Computer Science, 2024. https://doi.org/10.7717/peerj-cs.2128
[26] Bagdadee, Amam Hossain, et al. "Empowering smart homes by IoT-driven hybrid renewable energy integration for enhanced efficiency." Scientific Reports 15.1: 41491, 2025. https://doi.org/ 10.1038/s41598-025-25328-2
[27] Tawfik, Mohammed, et al. "Explainable few-shot learning with modern BERT for detecting emerging phishing attacks using XF PhishBERT: M. Tawfik et al." Scientific Reports 15.1: 42821, 2025. https://doi.org/ 10.1038/s41598-025-27500-0.
[28] Fathi, Islam S., and Mohammed Tawfik. "Enhancing IoT systems with bio-inspired intelligence in fog computing environments." Statistics, Optimization & Information Computing 13. , 2025. https://doi.org/ 10.19139/soic-2310-5070-2305.
[29] M. S. H. Lipu et al., "Micro energy harvesting for IoT platform: Review analysis toward future research opportunities," Heliyon, vol. 10, no. 6, Article e27778, Mar. 2024. 10.1016/j.heliyon.2024.e27778. https://doi.org/ 10.1016/j.heliyon.2024.e27778
[30] Al-Hazaimeh, Obaida M., et al. "Securing IoT Systems Using Artificial Intelligence-Driven Approaches." Statistics, Optimization & Information Computing 15.3: 1899-1912, 2026. https://doi.org/ 10.19139/soic-2310-5070-3342.
[31] A. K. Singh et al., "Development of IoT-enabled solutions for renewable energy generation and net-metering control for efficient smart home," Discover Internet of Things, vol. 4, Article 27, Sep. 2024. https://doi.org/ 10.1007/s43926-024-00065-6..
[32] A. Naouri et al., "Efficient fog node placement using nature-inspired metaheuristic for IoT applications," Cluster Computing, vol. 27, pp. 8225-8241, 2024. https://doi.org/ 10.1007/s10586-024-04409-3.
[33] Fathi, Islam S., et al. "Protecting IoT networks through AI-based solutions and fractional Tchebichef moments." Fractal and Fractional 9.7 : 427, 2025. 10.3390/fractalfract9070427. https://doi.org/ 10.3390/fractalfract9070427
[34] M. Zare, Y. E. Sola, and H. Hasanpour, "Imperialist competitive based approach for efficient deployment of IoT services in fog computing," Cluster Computing, vol. 27, pp. 845-858, 2024. https://doi.org/ 10.1007/s10586-023-03985-0
[35] A. Satouf, A. Hamidoglu, and O. M. Gul, "Metaheuristic-based task scheduling for latency-sensitive IoT applications in edge computing," Cluster Computing, 2024. https://doi.org/ 10.1007/s10586-024-04878-6

[36] R. Singh et al., "A hybrid meta-heuristic algorithm for multi-objective IoT service placement in fog computing environments," Internet of Things, vol. 23, Article 100973, Dec. 2023. https://doi.org/ 10.1016/j.iot.2023.100973
[37] Hassan, Gaber, et al. "Efficient compression of fetal phonocardiography bio-medical signals for Internet of Healthcare Things." IEEE Access 11: 122991-123003, 2023. https://doi.org/ 10.1109/ACCESS.2023.3329889
[38] A. Naghash Asadi et al., "Optimal deploying IoT services on the fog computing: A metaheuristic-based multi-objective approach," Journal of King Saud University - Computer and Information Sciences, vol. 35, no. 2, pp. 528-555, 2023. https://doi.org/ 10.1016/j.jksuci.2022.12.005
[39] D. Praveen Kumar and T. Amgoth, "A Hybrid and Light Weight Metaheuristic Approach with Clustering for Multi-Objective Resource Scheduling and Application Placement in Fog Environment," Expert Systems with Applications, vol. 227, Article 120229, 2023. https://doi.org/ 10.1016/j.eswa.2023.120229
[40] A. K. Maurya and R. Tripathi, "An integrated approach of ML-metaheuristics for secure service placement in fog-cloud ecosystem," Internet of Things, vol. 22, Article 100786, May 2023. https://doi.org/ 10.1016/j.iot.2023.100786
[41] F. Rossi et al., "Optimizing Service Replication and Placement for IoT Applications in Fog Computing Systems," in Euro-Par 2024: Parallel Processing, pp. 286-300, 2024. https://doi.org/ 10.1007/978-3-031-69583-4_20.
[42] Pinky et al., "Enhanced Task Scheduling With Metaheuristics for Delay and Energy Optimization in Cloud-Fog Computing," Concurrency and Computation: Practice and Experience, vol. 37, Article e8515, 2025. https://doi.org/ 10.1002/cpe.70163
[43] Tawfik, Mohammed, Amr H. Abdelhaliem, and Islam Fathi. "Quantum-Resistant Privacy-Preserving IoT Authentication via Zero-Knowledge Proofs and Blockchain Integration." Statistics, Optimization & Information Computing 14.3: 1374-1402, 2025. https://doi.org/ 10.19139/soic-2310-5070-2399
[44] Fathi, Islam S., et al. "Fractional Chebyshev Transformation for Improved Binarization in the Energy Valley Optimizer for Feature Selection." Fractal and Fractional 9.8: 521, 2025. https://doi.org/ 10.3390/fractalfract9080521
[45] Al-Shalabi, Mohammed, et al. "Optimal sizing of smart hybrid renewable energy system using Lotus Effect Optimization Algorithm." Energy Reports 14 (2025): 1936-1948. https://doi.org/ 10.1016/j.egyr.2025.08.007
[46] A. K. Al Hwaitat and H. N. Fakhouri, "The OX Optimizer: A Novel Optimization Algorithm and Its Application in Enhancing Support Vector Machine Performance for Attack Detection," Symmetry, vol. 16, no. 8, p. 966, 2024. https://doi.org/ 10.3390/sym16080966

Authors' Profiles

Islam S. Fathi received the B.Sc. and M.Sc. degrees in math and computer sciences from the Faculty of Science, Zagazig University, Egypt, in 2013 and 2019, respectively. He received his PhD degree in computer science, Faculty of Science, Suez Canal University, Egypt, in 2023. He is currently working as Assistant Professor of computer science (AI) in Faculty of Information Technology, Ajloun National University, JORDAN. His research interests include signal processing, metaheuristic optimization, bioinformatics, Artificial intelligence, and Internet of Things.

How to cite this paper:

Islam S. Fathi, "Green D-OXA: Energy-Efficient Fog Node Placement with Renewable Energy Integration for Sustainable IoT Networks", International Journal of Computer Network and Information Security(IJCNIS), Vol.18, No.3, pp. 1-22, 2026. DOI:10.5815/ijcnis.2026.03.01